Title: In-plane orthotropic behavior of timber floor diaphragms in unreinforced masonry buildings

Aaron Wilson[1]; Pierre J. H. Quenneville[2], M. ASCE; and Jason M. Ingham[3], M.ASCE

ABSTRACT

A full-scale experimental program consisting of testing four as-built diaphragms and four retrofitted diaphragms in both principal loading directions is presented. As-built configurations were typical of those found in historic unreinforced masonry buildings in North America and Australasia, while retrofitted diaphragms consisted of plywood panel overlays with stapled sheet metal blocking systems (SMBS). Test results were characterized using bilinear representations to establish recognizable performance parameters such as shear strength, shear stiffness, and ductility capacity, which were then used for comparative analysis. The nonlinear and low stiffness behavior of as-built diaphragms was confirmed in each principal loading direction. The plywood overlay and SMBS dramatically improved as-built diaphragm shear strength and shear stiffness, and were shown to perform satisfactorily from a serviceability perspective. The orthotropic nature of as-built diaphragms was proven, with perpendicular-to-joist shear stiffness being as low as 68% of the corresponding orthogonal value. A typical duly framed stairwell penetration and discontinuous joists with two-bolt lapped connections were shown to have no

[1] Ph.D. Graduate, Department of Civil & Environmental Engineering, The University of Auckland, Private Bag 92019, Auckland Mail Centre 1142, New Zealand, awil222@aucklanduni.ac.nz

[2] Professor, Department of Civil & Environmental Engineering, The University of Auckland, Private Bag 92019, Auckland Mail Centre 1142, New Zealand, p.quenneville@auckland.ac.nz

[3] Associate Professor, Department of Civil & Environmental Engineering, The University of Auckland, Private Bag 92019, Auckland Mail Centre 1142, New Zealand, j.ingham@auckland.ac.nz

detrimental impact on tested diaphragm performance. Predicted diaphragm performance using state-of-art assessment documents NZSEE (2006) and ASCE 41-06 (2007) was shown to be inconsistent with corresponding values established from testing. It is recommended that these assessment procedures be updated with revised performance parameters and provisions to address diaphragm orthotropic behavior.

CE Database subject headings: Brick Masonry; Diaphragms; Earthquakes; Experimentation; Floors; Retrofitting; Wood

INTRODUCTION

Unreinforced masonry (URM) buildings in North America and Australasia are typically constructed with rigid clay brick perimeter walls and comparatively light timber floor diaphragms. Such ‘western-style’ timber diaphragms typically comprise either straight-edge or tongue and groove floorboards nailed perpendicular to joists that span between URM walls. When the perimeter walls are spaced close enough (less than approximately 6.0 m), joists often span continuously between these elements. For larger spans, joists are lapped or butted over intermediate steel or timber cross-beams supported on columns or walls. Diaphragm blocking and chord elements are almost never present, and timber cross-bracing is usually fitted intermittently between joists to prevent out-of-plane buckling. Joist ends are typically either simply supported on a brick ledge (resulting from the perimeter walls reducing in width at each storey height), or are pocketed into the wall to a depth equal to one brick width.

Published research and earthquake reconnaissance reports have routinely highlighted the influence of timber diaphragm behavior on the seismic performance of URM buildings (Ingham et al. 2011; Simsir 2004; Tena-Colunga and Abrams 1996). Specifically, diaphragm flexibility and inadequate floor-to-wall anchorage have been considered the principal cause of many observed URM building earthquake failures (Bruneau 1994). Despite recognition of their importance, timber diaphragms have received little research attention. ABK (1981) and Peralta (2003; 2004) are perhaps the only seminal studies to have experimentally evaluated existing western-style diaphragm behavior, and to have examined possible retrofitting techniques to improve diaphragm performance. Other research initiatives, such as that published by Corradi (2006), Piazza et al. (2008a; 2008b), Brignola (2009), and Baldessari (2010), have also evaluated as-built and retrofitted diaphragm performance, but have focused primarily on Italian-style timber diaphragms that are unique to that region.

Published research has demonstrated that straight-sheathed diaphragms are nonlinear, flexible, and remain largely serviceable after undergoing large displacements. Diaphragm research, however, has focused almost exclusively on the parallel-to-joist loading direction, while orthotropic behavior has been largely ignored. This lack of experimental data has translated into assessment procedures (ASCE 2007; NZSEE 2006) that do not address or consider the orthotropic performance of timber floor diaphragms. Additionally, the effects of common diaphragm configuration features, such as the presence of stairwell penetrations or the presence of discontinuous joists, have yet to be suitably quantified and incorporated into current assessment procedures.

Numerous diaphragm retrofit solutions have been proposed over the past few decades. Particularly relevant is the provision of floorboards overlain or under hung at an angle to the existing framing, fiber reinforced polymer (FRP) lattice overlays, light gauge steel strap lattice overlays, reinforced concrete slab overlays, and under hung steel trusses (see for example ABK (1981), Peralta (2003), Corradi et al. (2006), and Baldessari (2010)). Many of these technologies provide advantageous performance, but are either too expensive for moderately valued URM buildings, or require invasive remedial works that render the retrofit undesirable from a construction perspective. Plywood overlay configurations have generally emerged as the preferred retrofitting technique due to an optimal trade-off between performance improvement and invasive construction requirements. There remains a need to establish a cost-effective and readily repeatable plywood retrofitting method that encourages the preservation of existing diaphragm construction.

Details of an experimental program that comprised full-scale testing of as-built and retrofitted diaphragm configurations in both principal loading directions are presented. The specific objectives of this research were to: (1) quantitatively establish the orthotropic performance characteristics of historic timber floor diaphragms in both principal loading directions (parallel-to-joists and perpendicular-to-joists), (2) determine the effects of penetrations and discontinuous joists on diaphragm performance, and (3) quantify the improvement of as-built diaphragm performance using a cost-effective retrofitting technique.

CONSTRUCTION OF FULL-SCALE DIAPHRAGMS

As-built test units

Four diaphragms representative of as-built conditions were constructed with new timber and new nails, and were assigned representative framing parameters to replicate as much as possible the typical existing diaphragm construction. Each diaphragm measured 10.4 m × 5.5 m and comprised 135 mm × 18 mm straight-edge timber floorboards fastened perpendicular to 45 mm × 290 mm MSG8 joists spaced at 400 mm centers. The joists were orientated parallel to the 5.5 m dimension, and the floorboards were orientated parallel to the 10.4 m dimension in an identical pattern to remove the influence that floorboard arrangement had on diaphragm performance. Two 3.15 mm (diameter) × 75 mm common bright roundhead nails were power driven at approximately 95 mm spacing to fasten the floorboards at each joist location. The ends of discontinuous joists in the same row were butted together at joist locations only, and each end was fastened with two nails as described above.

Two of the as-built diaphragms were tested parallel-to-joists and were designated as 1a-PARA and 2a-PARA. These two diaphragms were fitted with 45 mm × 75 mm timber cross-bracing at 1/3 joist length locations to replicate typical restraint against lateral joist buckling. 1a-PARA was a homogeneous configuration with no openings. 2a-PARA featured a 3.2 m × 1.0 m corner penetration to evaluate the effect that a typical stairwell opening may have on diaphragm performance. Although it is acknowledged that stairwell penetrations may also influence diaphragm performance perpendicular-to-joists, only a limited number of tests were available due to finite resources, so not all possible penetration configurations could be studied.

The remaining two as-built diaphragms were tested perpendicular-to-joists, and were designated as 1a-PERP and 2a-PERP. For these two diaphragms the cross-bracing was replaced with full-depth blocking at the locations of load application, to effectively transmit applied quasi-static loads into the diaphragm. The provision of full-depth blocking for diaphragms tested perpendicular-to-joist would not have affected orthotropic performance comparison, as inter-joist framing merely provides lateral restraint for diaphragms loaded parallel-to-joist. Diaphragm 1a-PERP was considered to be homogeneous with complete sheathing and continuous joists spanning between their supports. To quantify the influence that discontinuous joists may have on diaphragm performance, 2a-PERP comprised discontinuous joists with a typical two-bolt lapped connection at diaphragm midspan, while all other configuration parameters remained identical to 1a-PERP. Local movement at the joist splices was not explicitly measured but rather splice integrity was gauges by overall diaphragm performance.

It is acknowledged that testing multiple diaphragms of each configuration type is desirable to address behavior variability. However despite this recognition, the construction and testing of multiple full-scale diaphragms of equivalent configuration was unfortunately not possible within the available budget. The presented test results therefore provide an important indication of penetrations and joist splices on diaphragm performance, but further testing may be required to thoroughly validate these findings.

The configuration characteristics of the tested as-built diaphragms are illustrated in Fig. 1a and outlined in Table 1. The geometrical configuration of 2a-PARA is shown to illustrate the dimensions of the corner stairwell penetration.

Retrofitted test units

After each as-built diaphragm was tested, a plywood overlay and stapled sheet metal blocking retrofit system was applied, and the diaphragm was re-tested using an identical testing methodology. As discussed previously, the plywood overlay retrofit strategy was adopted because it has emerged as a popular and cost-effective retrofit technique that provides suitable diaphragm performance improvement. Given that existing diaphragms in URM buildings are almost always constructed of timber, the implementation of plywood and other timber members to strengthen the diaphragm is comparatively simple. The plywood sheets can be fastened either over the existing floorboards, or to the underside of the floor as a 'ceiling' diaphragm, depending on aesthetic requirements. The stapled sheet metal blocking system (SMBS) provides the necessary transfer of shear flow between plywood panels and eliminates the need for conventional blocking that involves nailing timber framing between joists along plywood panel boundary lines. The less invasive nature of this retrofit allows existing diaphragm materials to be retained and promotes the preservation of architectural heritage. The purpose of the plywood overlay and SMBS was therefore to quantify the improvement in diaphragm performance using a cost-effective and repeatable retrofitting method that encourages the preservation of existing diaphragm construction.

The retrofit system was designed using the provisions of the New Zealand Timber Structures Standard NZS 3603:1993 and by utilizing stapled sheet metal blocking test results published by Holmes Solutions Ltd (Oliver 2008). Retrofit strength and stiffness were formulated against 1/500 year return period design earthquake loads that were determined in accordance with NZS 1170.5:2004 by assuming a two-storey URM building located in Wellington, New Zealand, with dimensions of 10.4 m long × 5.5 m wide × 7.0 m high. The design earthquake loads were parabolically distributed across the diaphragm in accordance with ASCE 41-06 (2007). The performance contribution of the existing framing was neglected during retrofit design. Comprehensive details of the design procedure can be found in Wilson (2012).

The retrofitted diaphragms were designated as 1b-PARA, 2b-PARA, 1b-PERP, and 2b-PERP, corresponding to the relevant as-built configuration. All retrofits consisted of 2400 mm × 1200 mm × 15 mm AS/NZS 2269:2004 structural grade plywood laid over the existing floorboards with 75 mm × 24 gauge sheet metal straps fastened to the plywood edges with ECKO SF-9215 staples at 100 mm centers. The staple wire had a rectangular cross-section of 1.24 mm × 1.00 mm and a leg length of 15 mm. Field nailing (approximately 300 mm centers) was applied to the plywood sheets at the locations of the joists to mitigate buckling of the panels during large diaphragm displacements, while nailing was provided at 100 mm centers around all diaphragm edges to effectively transfer shear forces. All nails were 3.15 mm (diameter) × 75 mm roundhead power driven nails.

Each retrofitted diaphragm was fitted with chords to resist the tension and compression forces generated during lateral deformation. Compression chords for 1b-PARA and 2b-PARA were introduced by nailing full-depth blocking between the joists, while tension chords comprised 40 mm × 6 mm mild-steel flats fastened to the timber blocking with 75 mm × 10 gauge screws at 100 mm centers.

1b-PERP and 2b-PERP did not require the blocking and steel flat chord elements provided in 1b-PARA and 2b-PARA, as the continuous joists at each end of the diaphragm could be utilized as chord members. Edge nailing provided at 100 mm centers was shown by design to sufficiently engage the joists as combined compression and tension chords. Full-depth blocking was fastened between the joists along the sides of the diaphragm to provide a consistent line of framing for diaphragm edge nailing and for effective shear transfer.

The general retrofit configuration described above is illustrated in Fig. 1b and outlined in Table 1. The additional retrofit details required for 2b-PARA to address the increased stress concentrations surrounding the corner penetration are also provided.

TEST DETAILS

Test set-up for loading parallel-to-joists

The test set-up for diaphragms loaded parallel-to-joists is shown in Fig. 2a. Loading was provided by a single hydraulic actuator connected to a large box-frame that was anchored to the concrete floor with fifteen epoxied studs and that had two 1-tonne concrete slabs on top of it to ensure rigid reaction against the applied loads. A distribution frame comprising a primary truss structure and two secondary beams on castors was used to distribute the actuator point load into four equal loads that were applied to the diaphragm at joist locations. The primary truss, secondary beams and joist loaders were connected with purpose-built hinge joints that enabled the secondary beams to rotate with the deforming diaphragm, and to ensure that applied loading was free of any induced moments. Reversed cyclic loading was achieved by positioning loaders on both ends of the loaded joists and post-tensioning these together using M16 threaded rods that spanned the length of the diaphragm. The distributed loading mechanism was a practical replication of diaphragm earthquake loading, which involves the inertial mass of the out-of-plane walls being transmitted into the diaphragm through its joists. Additionally, the locations of applied load were selected to best simulate the parabolic load distribution recommended by ASCE 41-06 (2007).

To provide the necessary restraint against lateral loading, the two side-joists were fastened to inverted T-sections fabricated from 6.0 m long steel plates. Holes were drilled in the side joists at twelve prefabricated bolt-hole locations in the T-section web and M16 bolts were used to create a tight friction connection between the steel and timber to prevent any lateral slip from occurring. The T-sections were anchored to the concrete floor of the warehouse using M16 studs and high strength epoxy mortar to completely fix against movement.

Beams made of 150 UB 14 steel sections were bolted to the concrete slab and blocked with timber to provide vertical support at the joist ends. This intermediate support was necessary as the floorboards spanning between the two fixed side-joists could not carry the self-weight of the diaphragm. Teflon pads were fastened to the supports at joist locations to minimize friction resistance to diaphragm displacement.

Test set-up for loading perpendicular-to-joists

The test set-up for diaphragms loaded perpendicular-to-joists is shown in Fig. 2b. Due to a considerable reduction in diaphragm span, the loading system used for diaphragms tested parallel-to-joists was reconfigured for two points of loading, instead of four, by removing the secondary beams and connecting the joist loaders directly to the primary truss. Again, the locations of applied load were selected to represent a parabolic load distribution (ASCE 41-06 2007), while reversed-cyclic loading was again achieved by post-tensioning loaders at each end of the diaphragm.

Two URM walls measuring approximately 600 mm high × 230 mm wide × 11500 mm long were constructed to provide lateral support against applied diaphragm loading whilst providing realistic boundary conditions for the joists. The walls were constructed with solid clay bricks recycled from a heritage URM building in Auckland and a mortar composition of one part cement to one part lime to six parts sand (1:1:6 mortar). Material testing of URM walls was not a focus of this research but has been comprehensively reported in Lumantarna et al. (2012a; 2012b). Overall the walls were six bricks high, two bricks wide and approximately 11.5 m long. Diaphragm joists were seated in pockets that were one brick deep and approximately 49 mm wide, and were provided at 400 mm centers along the URM walls, which replicated a typical joist seating condition found in many existing URM buildings. It is acknowledged that a common practice in some countries was to pack the joist pockets with mortar, grout, or even construction debris. It is logical to assume that such joist pocket packing would improve diaphragm performance in the perpendicular-to-joist direction, by providing some level of moment fixity to the joist ends. To investigate this issue comprehensively, it would be necessary to perform multiple tests with varying levels of mortar packing to quantify its influence. However because this detail was not a principal focus of the study, a decision was made to consider only the worst case scenario with no mortar present. The brick walls were also post-tensioned to the warehouse concrete slab to generate sufficient shear strength within the walls and to generate sufficient friction resistance between the walls and the concrete slab to prevent sliding from occurring.

Beams made of 150 UB 14 steel sections with timber blocking were also bolted to the concrete floor of the warehouse to provide vertical support for the discontinuous joists at midspan. This detail replicated typical diaphragm support conditions where discontinuous joists are seated on intermediate timber or steel cross-beams that are supported on columns.

Instrumentation and test procedure

The instrumentation used to capture essential diaphragm response in each principal loading direction is illustrated in Fig 2. During each test, total load ‘F’ was recorded using a load cell attached to the actuator, while the diaphragm deformation profile was measured at three locations ‘DISP1’, ‘DISP2’ and ‘DISP3’ using string potentiometers.

Each diaphragm was subjected to quasi-static reversed-cycle loading to midspan displacement amplitudes of 2.5 mm, 5 mm, 15 mm, 25 mm, 50 mm, 75 mm, 100 mm and 150 mm. Each displacement amplitude was repeated three times to investigate the cyclic degradation of diaphragm performance. Once this loading schedule had been completed, an attempt was made to push and pull the diaphragm to the maximum stroke of the actuator, which was ±150 mm. Because it was difficult to set the actuator perfectly at the centre of its stroke, the maximum negative displacement generally exceeded the maximum positive displacement. Loading was applied at an average rate of 20 mm/min. The push direction was defined as positive and the pull direction was defined as negative.

TEST RESULTS

As-built diaphragms demonstrated low stiffness with no indications of structural failure up to drifts of 3.8% and 5.4% in the parallel-to-joist and perpendicular-to-joist loading directions, respectively. Drift is defined as the ratio between midspan displacement and half diaphragm span. All as-built diaphragms therefore exhibited no residual damage and remained completely serviceable at the conclusion of testing. The mechanism for diaphragm deformation appeared to be flexural bending of the floorboards (for parallel-to-joist loading) or joists (for perpendicular-to-joist loading), which was resisted by induced shear deformation of the floorboard-to-joist nail connections. Wilson (2013) demonstrated that this complex interaction of framing deformation and intermittent nail couple rotation is most suitably captured by a shear beam idealization. The absence of side frame rotation during testing (see below) also confirms that overall diaphragm deformation is governed by shear-type response.

The presence of a corner penetration in 2a-PARA appeared to not alter diaphragm behavior in the parallel-to-joist direction. As-built diaphragms tested perpendicular-to-joists (1a-PERP and 2a-PERP) responded identically when subjected to lateral loading, indicating that the discontinuous joists with bolted lapped connections in 2a-PERP did not adversely affect diaphragm behavior. Joist ends were observed to rotate freely within the oversized URM wall pockets up to midspan displacements of approximately ±50 mm, after which some prying actions occurred.

Overall, the plywood overlay and sheet metal blocking retrofit performed well up to 0.5% drift, but displayed potential serviceability issues above 1.4% drift with considerable plywood panel distortion that compromised the finished floor and that would require considerable remedial work to rectify. Comprehensive test observations for both as-built and retrofitted diaphragms are reported in Wilson (2012).

It is important to acknowledge that diaphragm uplift, side frame rotation (for parallel-to-joist direction), URM side wall movement (perpendicular-to-joist direction), and reaction block deformation did not occur during testing. As shown in Fig. 2, strain 'portal' gauges were used to measure the in-plane and out-of-plane displacement of the steel side frames during parallel-to-joist testing. The recorded displacements from all transducers were negligible, which confirms that steel side frame rotation did not occur (see Wilson 2012). Although the remaining deformations were not measured electronically, reference markers were positioned and visually monitored during each test to ensure that diaphragm uplift, URM side wall movement, and reaction block deformation did not occur. The implications of these observations are important because it means that the force-displacement data presented in the following section did require modification to determine relative diaphragm response.

Force-displacement response

The force-displacement response of as-built diaphragms and their corresponding retrofitted configurations are presented in Fig. 3 for comparison. Due to the significant differences in as-built and retrofitted diaphragm load resistance, it is difficult to fully observe as-built diaphragm response. Fig. 4 provides a refined plot of positive-only displacements of 1a-PARA backbone curve, to better illustrate as-built diaphragm response. Fig. 4 shows that as-built diaphragms exhibited nonlinear characteristics up to displacements of approximately 25 mm, beyond which diaphragm response was essentially linear. This nonlinearity is derived from nail yielding and localized timber crushing where the embedded nail shank is forced into contact with the surrounding timber (Dean et al. 1989). However, despite this non-recoverable strength loss, it is evident that no clearly defined yield point exists. The force-displacement responses display no indication of strength degradation, which confirms diaphragm flexibility and the absence of observed structural failures during testing. Only small strength losses are evident between cycles one, two and three at each displacement amplitude, indicating that as-built diaphragm performance does not significantly degrade when repeatedly loaded to the same displacement.

For retrofitted diaphragms, significant differences are observable between initial stiffness and secondary stiffness, making an effective yield point more distinguishable. The comparatively high initial stiffness is attributable to the stapled sheet metal blocking system that effectively transferred shear flow between plywood panels up to drifts of approximately 0.5%, after which the majority of staples became ineffective, causing reduced shear transfer between plywood panels and a reduction in overall diaphragm stiffness.

Diaphragms 1b-PARA and 2b-PARA demonstrated strength integrity up to drifts of 1.9%, after which strength reductions occurred, while diaphragms 1b-PERP and 2b-PERP showed no overall strength degradation. Unlike the as-built configurations, which exhibited negligible strength reduction when repeatedly loaded to the same displacement, retrofitted diaphragm test results showed an average percentage strength reduction of approximately 14% between of the first and third loading cycles.

Performance characterization

Essential diaphragm force-displacement performance can be captured using a bilinear idealization of the backbone response curve. Fig. 5 illustrates key diaphragm performance parameters for as-built and for retrofitted diaphragms, such as initial stiffness K_1, secondary stiffness K_2, yield load F_y, and corresponding yield displacement Δ_y. As reported by Peralta (2004), bilinear representations can be constructed by applying the principle of hysteretic energy conservation (Mahin and Berterto 1981). To solve the energy conservation equation for as-built diaphragms, the following constraints were applied to the bilinear curve: (1) must pass through zero load and zero displacement, (2) secondary stiffness was taken as the average gradient of the linear portion of displacement amplitudes above 50 mm, and (3) final displacement, F_{max}, was taken as the maximum displacement of the linear portion of displacement amplitudes above 50 mm. In the absence of a universally accepted procedure to characterize the nonlinear behavior of unretrofitted timber diaphragms, the 50 mm displacement amplitude constraint was adopted because the gradient of the backbone curves were essentially linear after this point. The bilinear curve generated for diaphragm 1a-PARA is shown in Fig. 4, which demonstrates that as-built diaphragm force-displacement response can be suitably captured by a bilinear representation. Retrofitted diaphragm performance was characterized in accordance with ASTM standard E2126 (2010), which is also based on the hysteretic energy conservation principle, but which stipulates an elastic-perfectly plastic bilinear representation.

Diaphragm strength is conventionally reported as shear strength per lineal meter width of the diaphragm, R_d, which removes the influence of diaphragm geometry. For each diaphragm, shear strength was calculated by taking the relevant bilinear yield load, halving it to find shear resistance, and dividing it by the width of the diaphragm (B), as described in Eq. 1.

$$R_d = \frac{F_y}{2B} \tag{1}$$

Diaphragm stiffness, K_d, is considered to be initial stiffness, K_1, shown in Fig. 5, for diaphragm seismic assessments. Diaphragm stiffness is conventionally converted to shear stiffness, G_d, to achieve independence from diaphragm geometry, and to allow comparison of varying configurations. For the diaphragms tested parallel-to-joists (four-point loads), it can be shown that shear stiffness is determined using Eq. 2 below:

$$G_d = \frac{K_d\left(a + \frac{b}{2}\right)}{2B} \tag{2}$$

where a is the distance from the side of the diaphragm to the first point load and b is the distance between the first and second point loads. Eq. 2 also applies to diaphragms tested perpendicular-to-joists (two-point loads) but in which case $b = 0$.

The as-built and plywood-retrofitted diaphragms demonstrated ductile behavior by undergoing large deformations without significant strength degradation. Ductility capacity is typically defined by Eq. 3, which is formulated based upon the equal displacements principle of elastic-perfectly plastic behavior (Park et al. 1987).

$$\mu = \frac{\Delta_{ult}}{\Delta_y} \tag{3}$$

Fig. 3 shows that ultimate displacement was not captured during as-built diaphragm testing, meaning that ductility capacity could not be calculated explicitly from test results. In order to gauge some level of diaphragm ductility capacity, Eq. 3 was applied by taking the maximum recorded displacement value of each as-built test as the ultimate displacement and the corresponding yield displacement determined from the bilinear idealizations. Despite using conservative definitions, ductility capacity was found to be between 6.7 and 8.9 for as-built diaphragms, which considerably exceed the typical values published in earthquake loading standards such as AS/NZS 1170 (2002) that recommend a maximum ductility capacity of $\mu = 6$. Extrapolation of the force-displacement response to estimate ultimate displacement was therefore considered unnecessary.

The performance parameters determined above for as-built and retrofitted diaphragms are presented in Table 2 for comparison.

DISCUSSION

Retrofit performance

The plywood overlay and stapled sheet metal blocking retrofit was proven to significantly improve as-built diaphragm performance in both principal loading directions, as shown in Fig. 3 and summarized in Table 2. The shear strength (R_d) and shear stiffness (G_d) values determined for retrofitted diaphragms tested parallel-to-joists were up to 9.9 and 22.9 times greater than the corresponding values determined for as-built configurations, respectively. An analogous comparison for diaphragms tested perpendicular-to-joists shows that the shear strength and shear stiffness values determined for retrofitted diaphragms were up to 7.5 and 17.2 times greater than their corresponding as-built configurations, respectively. Such prodigious performance improvements from plywood overlay retrofits is consistent with published research such as Johnson (1971), ABK (1981), and Peralta (2004).

It is evident from the performance parameters described above that the magnitude of performance improvement was greater for retrofitted diaphragms tested parallel-to-joists than for retrofitted diaphragms tested perpendicular-to-joists. This retrofit performance discrepancy is most likely associated with plywood panel orientation. Given the orientation of the existing floorboards beneath the overlay, the constructed overlays caused localized shear flow weaknesses that were particularly evident in diaphragms tested perpendicular-to-joists, therefore generating a slightly lower relative performance improvement than for diaphragms tested parallel-to-joists. Based on this performance observation, it is recommended that when undertaking diaphragm retrofit design, engineering practitioners consider carefully which principal direction requires the greatest performance enhancement, and designate the plywood panel orientation accordingly.

The efficacy of a retrofit system is not only measured by improved stiffness and strength, but also by the enduring serviceability of the diaphragm during and after earthquake loading. To establish whether the potential serviceability issues observed during testing would occur during a design earthquake, diaphragm displacement demand was determined for design elastic earthquake loading and compared against the observed midspan displacements that caused the sheet metal straps and plywood panels to begin buckling. Sheet metal buckling and plywood buckling have been labeled as serviceability limits Δ_{L1} and Δ_{L2}, respectively, and are shown in Table 3. The serviceability limits were determined during the tests through observations (not calculations), whereas the displacement demands were calculated using Eqs. 4 and 5 below.

$$\mu_{demand} = \frac{F_e}{F_y} \tag{4}$$

$$\Delta_{demand} = \mu_{demand} \times \Delta_y \tag{5}$$

Where μ_{demand} is ductility demand, F_y is effective yield load defined by the idealized bilinear response curve outlined in Table 2, and F_e is the design elastic earthquake load, determined from the provisions of NZS 1170.5 (2004) for a 1/500 year return period, assuming $\mu = 1.0$ and based on a typical two-storey URM building. The calculated values are outlined in Table 3 and illustrated in Fig. 6.

By comparing the design earthquake displacement demands with the experimentally observed serviceability limits presented in Table 3, it can be established that at peak displacement arising from a design level earthquake (as per NZS 1170.5:2004), considerable sheet metal buckling and staple pullout would be expected for diaphragms loaded parallel-to-joists, with less damage expected for loading perpendicular-to-joists. The displacements necessary to cause plywood buckling and uplift are shown to be unlikely for both principal loading directions, as displacement demands are less than one third of the observed upper serviceability limits.

Overall, the plywood overlay and SMBS is a unique retrofitting method that allows the preservation of existing diaphragm materials (see Fig. 1b). This retrofit technique was shown to significantly increase diaphragm stiffness and strength in both principal loading directions, but is likely to suffer serviceability issues associated with the buckling of sheet metal straps and pullout of stapling when subjected to a design level earthquake. Depending on the in-service use of the floor diaphragm, the reinstatement of the SMBS could be troublesome if internal partitions and heavy office furniture exist, and is therefore an important retrofit design consideration.

Orthotropic behavior

The performance of timber floor diaphragms was shown to be distinctly different in the principal loading directions parallel-to-joists and perpendicular-to-joists. This orthotropic behavior was expected from the orthogonal arrangement of floorboards and joists in the as-built diaphragm configurations. Although shear strength was similar for as-built diaphragms in both loading directions, shear stiffness was shown to be up to 32% less for loading perpendicular-to-joists. This dissimilarity was further exaggerated for retrofitted diaphragms, with a reduction in shear stiffness of up to 60% between the parallel- and perpendicular-to-joist loading directions. Shear strength was also reduced from approximately 16 kN/m in the direction parallel-to-joists, to approximately 9.5 kN/m in the direction perpendicular-to-joists.

Effect of stairwell penetration

Comparing the force-displacement responses of diaphragms 1a-PARA and 2a-PARA in Fig. 3, the presence of a corner penetration equal to approximately 6% of the floor area appeared to have little effect on diaphragm performance. The values listed in Table 2 show that shear strength is unchanged and that shear stiffness is marginally reduced from 198 kN/m to

185 kN/m. These results indicate that a typical single-case stairwell opening is not significantly detrimental to as-built diaphragm performance in the loading direction parallel-to-joists.

Retrofitted diaphragms 1b-PARA and 2b-PARA also responded similarly to lateral loading, although shear strength and shear stiffness were slightly reduced for 2b-PARA (see Table 2). This is contrary to the findings of Kamiya (1998) who reported that ultimate strength was equal for three tested plywood diaphragms, regardless of the presence of a penetration. The observed performance reduction highlights the importance of incorporating specific retrofitting details immediately adjacent to penetrations. Without the additional chord member, and increased stapling and nailing provided in the vicinity of the corner penetration, retrofitted diaphragm 2b-PARA may have performed more poorly than that which was tested.

Effect of discontinuous joists

The lapped and bolted joist connections in diaphragms 2a-PERP and 2b-PERP were observed to suffer no damage during testing, even at midspan displacements of ±150 mm. Surprisingly, using the adopted force-displacement characterization methodologies, shear strength and shear stiffness were found to be higher for 2a-PERP than 1a-PERP (see Table 2). For retrofitted diaphragms shear strength slightly decreased but shear stiffness dramatically increased between 1b-PERP and 2b-PERP. These results were unexpected as diaphragm response perpendicular-to-joists seemingly relies heavily on the out-of-plane flexural capacity of the joists, which would be expected to reduce for discontinuous joists with only a two-bolt lapped connection. However, it is possible that the diaphragm action of the floorboards, combined with the two-bolt lapped joist connections was sufficient to resist the induced joist bending moments and not compromise diaphragm performance. The described performance discrepancy is therefore possibly due in part to construction or material variability. Nevertheless the test results suggest that discontinuous joists with reliable mechanical connections do not adversely affect diaphragm performance.

Comparison with current assessment procedures

Desktop assessment procedures aid structural engineers by transforming complex loading and response mechanisms into quantifiable performance parameters that can be used for design. It is understood that New Zealand practitioners currently refer to the NZSEE (2006) and ASCE 41-06 (2007) documents to perform seismic assessments of heritage timber floor diaphragms. To verify the accuracy of the assessment procedures published in these documents, predicted values of diaphragm yield strength, yield displacement, and stiffness were compared against experimentally determined values for as-built configurations, and are summarized in Table 4.

The values listed in Table 4 illustrate that diaphragm performance parameters are either under predicted or over predicted using the NZSEE and ASCE 41-06 assessment procedures. Yield strength was generally well predicted for parallel-to-joist loading but discrepancies of up to 35% were shown for perpendicular-to-joist loading. Diaphragm yield displacement was grossly over predicted using the methodology in NZSEE, while yield displacement was either over or under predicted using the ASCE 41-06 guidelines. Predicted diaphragm stiffness was as low as 30% of experimentally determined values using NZSEE guidelines. The reverse was true using ASCE 41-06 guidelines, where predicted diaphragm stiffness was 160% of corresponding values determined from testing.

It is evident from the comparison above that current assessment procedures poorly predict as-built diaphragm performance. It is recommended that existing assessment documents NZSEE (2006) and ASCE 41-06 (2007) be updated to reflect the performance parameters determined from this research. In addition, it is evident that current assessment documents offer no provisions to address orthotropic diaphragm behavior, which has been shown to be significant. In order to improve the transparency and accuracy of the assessment procedures, diaphragm performance parameters should be explicitly provided for in each principal direction.

LIMITATIONS AND RECOMMENDED RESEARCH

The principal limitation of the presented research is that tested diaphragms were constructed with new timber and new nails, while the effects of historic construction materials and decades, or even centuries, of service-life were ignored. Although the adopted configurations were representative of historic construction, there remains considerable motivation to quasi-statically and dynamically test full-scale timber diaphragms from existing heritage URM buildings, either by extraction or by testing in-situ.

In addition to testing heritage diaphragms, it is recommended that future research focus on the relationship between diaphragm stiffness and URM building seismic response. This should include system-level testing and modeling of URM buildings with diaphragms of varying stiffness and configuration. The objective of such research should be to formalize a performance-based design framework that enables structural engineers to optimize diaphragm stiffness for improved URM building seismic performance.

CONCLUSIONS

Quasi-static testing of full-scale timber floor diaphragms in both principal loading directions is, to the best of the authors' knowledge, the first of its kind. The nonlinear and low strength and low stiffness nature of as-built diaphragms was confirmed. As a result of their flexibility, as-built diaphragms exhibited no strength degradation up to drift ratios of 3.8% and 5.4% in the parallel-to-joist and perpendicular-to-joist loading directions, respectively. Published earthquake reconnaissance reports have emphasized that such diaphragm flexibility was the principal cause of many observed URM building earthquake failures.

The plywood overlay and SMBS retrofit dramatically improved as-built diaphragm strength and stiffness. The displacement demand for a typical 1/500 year return period earthquake demonstrated that serviceability issues associated with the buckling of sheet metal blocking would likely occur, but that the displacement levels required to cause plywood panel uplift would not be reached. If failure of the SMBS is considered to be acceptable performance, the results indicate that plywood panel overlay with SMBS is an effective retrofitting technique that can be implemented into current URM building stock whilst preserving heritage diaphragm construction. To ensure the best possible performance, it is recommended that the plywood overlay panels be orientated parallel-to-joists to avoid localized shear flow weaknesses.

Testing in both principal loading directions confirmed the orthotropic nature of timber diaphragms. While shear strength remained consistent for as-built diaphragms, shear stiffness in the direction perpendicular-to-joists was up to 32% less than the corresponding value in the orthogonal configuration. For retrofitted diaphragms, the difference in shear stiffness increased to 60%, and the shear strength in the direction perpendicular-to-joists was almost 50% of the shear strength parallel-to-joists.

Test results indicate that a typical stairwell penetration has an insignificant influence on as-built diaphragm performance, having almost no effect on shear strength, and only reducing shear stiffness from 198 kN/m to 185 kN/m. The almost identical response of diaphragms 1b-PARA and 2b-PARA demonstrated that additional retrofitted details are necessary adjacent to corner penetrations to maintain desired performance.

Discontinuous joists with a midspan, two-bolt lapped connection were shown to have no detrimental impact on diaphragm performance. These test results suggest that discontinuous joists with a reliable mechanical connection do not adversely affect diaphragm performance, however further testing is required to substantiate this finding.

A comparison of predicted diaphragm yield strength, yield displacement, and stiffness indicates that the NZSEE and ASCE 41-06 procedures are inconsistent and both poorly predict diaphragm performance. To improve accuracy, it is recommended that the assessment procedures be updated with representative values and that provisions be included for each principal loading direction to address the proven highly orthotropic nature of timber diaphragms.

ACKNOWLEDGEMENTS

The authors wish to acknowledge the financial support provided by the New Zealand Foundation for Research Science and Technology (FRST) grant UOAX0411. The tireless assistance of Nikolaus Hollwegs, Mark Byrami, and Jeffrey Ang throughout the experimental program is also gratefully appreciated.

REFERENCES

ABK. (1981). "Methodology for mitigation of seismic hazards in existing unreinforced masonry buildings: Diaphragm testing." *ABK-TR-03*, National Science Foundation, El Segundo, California.

ASCE. (2007). *Seismic rehabilitation of existing buildings, ASCE/SEI 41-06*, American Society of Civil Engineers, Reston, Va.

ASTM. (2010). "Cyclic (reversed) load test for shear resistance of vertical elements of the lateral force resisting systems for buildings." *ASTM E2126-10*, ASTM International.

Baldessari, C. (2010). "In-plane behaviour of differently refurbished timber floors," Ph.D. thesis, The University of Trento, Trento, Italy.

Brignola, A. (2009). "Evaluation of the in-plane stiffness of timber floors for the performance-based retrofit of URM buildings," Ph.D. thesis, University of Genoa, Italy.

Bruneau, M. (1994b). "State-of-the-art report on seismic performance of unreinforced masonry buildings." *Journal of Structural Engineering*, 120(1), 230-251.

Corradi, M., Speranzini, E., Borri, A., and Vignoli, A. (2006). "In-plane shear reinforcement of wood beam floors with FRP." *Composites Part B: Engineering*, 37(4-5), 310-319.

Dean, J. A., Deam, B. L., and Buchanan, A. H., (1989). “Earthquake resistance of timber structures.” *New Zealand Journal of Timber Construction*, 5(2), 12-16.

Ingham, J. M., Biggs, D. T., and Moon L. M. (2011). “How did unreinforced masonry buildings perform in the February 2011 Christchurch earthquake.” *The Structural Engineer*, 89(6), ISSN 1466-5123.

Johnson, J. W. (1971). “Lateral test of a 20- by 60-foot roof section sheathed with plywood overlaid on decking.” *Report T-29*. Oregon School of Forestry.

Kamiya, F., and Itani, R. Y. (1998). “Design of wood diaphragms with openings.” *Journal of Structural Engineering*, 124, 839-48.

Lumantarna, R., Biggs, D. T., and Ingham J. M. (2013a). “Compressive, flexural bond and shear bond strengths of in-situ New Zealand unreinforced clay brick masonry constructed using lime mortar between the 1830 and 1940s’.” *ASCE Journal of Materials in Civil Engineering*, in press.

Lumantarna, R., Biggs, D. T., and Ingham J. M. (2013b). “Uniaxial compressive strength and stiffness of field extracted and laboratory constructed masonry prisms.” *ASCE Journal of Materials in Civil Engineering*, in press.

Mahin, S. A., and Bertero, V. V. (1981). "An evaluation of inelastic seismic design spectra." *Journal of the Structural Division*, 107(ST9), 1777-1795.

New Zealand Society for Earthquake Engineering (NZSEE). (2006). *Assessment and improvement of the structural performance of buildings in earthquakes*, New Zealand Society for Earthquake Engineering, Wellington, New Zealand.

Park, T. Y., Reinhorn, A. M., and Kunnath, S. K. (1987). "IDARC: Inelastic damage analysis of reinforced concrete frame-shear wall structures." *Technical Report NCEER-87-0008*, National Center for Earthquake Engineering Research, State University of New York, Buffalo, New York.

Oliver, S. (2008). “Structural load testing of flooring diaphragm connection details.” *Report 102904.00 – 2.01*, Holmes Solutions Ltd, Christchurch.

Peralta, D. F. (2003). "Seismic Performance of Rehabilitated Wood Diaphragms," Ph.D. thesis, Texas A&M University, College Station, Texas.

Peralta, D. F., Bracci, J. M., and Hueste, M. B. D. (2004). "Seismic behavior of wood diaphragms in pre-1950s unreinforced masonry buildings." *Journal of Structural Engineering*, 130(12), 2040-2050.

Piazza, M., Baldessari, C., and Tomasi, R. (2008a). "The Role of In-Plane Floor Stiffness in the Seismic Behaviour of Traditional Buildings." 14th World Conference on Earthquake Engineering, Beijing, China, 12-17 October.

Piazza, M., Baldessari, C., Tomasi, R., and Acler, E. (2008b). "Behaviour of refurbished timber floors characterised by different in-plane stiffness." Proc. of Structural Analysis of Historic Construction, Bath, United Kingdom, 2-4 July.

Salenikovich, A. (2000). "The racking performance of light-frame shear walls," Ph.D. thesis, Virginia Polytechnic University and State University, Blacksburg, VA.

Simsir, C. C. (2004). "Influence of diaphragm flexibility on the out-of-plane dynamic response of unreinforced masonry walls," Ph.D. thesis, University of Illinois, Urbana-Champaign, USA.

Standards Association of New Zealand. (1993). “NZS 3603:1993, Timber Structures.” Standards New Zealand, Wellington, New Zealand

Standards Association of New Zealand. (2002). "AS/NZS 1170.1:2002, Structural Design Actions Part 0: General Principles." Standards New Zealand, Wellington, New Zealand.

Standards Association of New Zealand. (2004). "NZS 1170.5:2004, Structural Design Actions Part 5: Earthquake actions - New Zealand." Standards New Zealand, Wellington, New Zealand.

Tena-Colunga, A., and Abrams, D. P. (1996). "Seismic behavior of structures with flexible diaphragms." *Journal of Structural Engineering*, 122(4), 439-445.

Wilson, A. W. (2012). "Seismic Assessment of Timber Floor Diaphragms in Unreinforced Masonry Buildings," Ph.D. thesis, University of Auckland, New Zealand, accessed at: https://researchspace.auckland.ac.nz/handle/2292/14696.

Wilson, A., Quenneville, P., and Ingham, J. (2013). "Natural Period and Idealization of Flexible Timber Diaphragms." *Earthquake Spectra*, 29(3), in press.

LIST OF TABLES

TABLES

TABLE 1: Test matrix

Test reference	Loading direction	Dimensions	State	Feature
1a-PARA	Parallel-to-joists	10.4 m × 5.5 m	As-built	Homogeneous
1b-PARA	Parallel-to-joists	10.4 m × 5.5 m	Retrofitted	Homogeneous
2a-PARA	Parallel-to-joists	10.4 m × 5.5 m	As-built	Corner penetration
2b-PARA	Parallel-to-joists	10.4 m × 5.5 m	Retrofitted	Corner penetration with specific retrofitting
1a-PERP	Perpendicular-to-joists	5.5 m × 10.4 m	As-built	Homogeneous
1b-PERP	Perpendicular-to-joists	5.5 m × 10.4 m	Retrofitted	Homogeneous
2a-PERP	Perpendicular-to-joists	5.5 m × 10.4 m	As-built	Discontinuous joists with bolted lapped connection
2b-PERP	Perpendicular-to-joists	5.5 m × 10.4 m	Retrofitted	Discontinuous joists with bolted lapped connection

TABLE 2: Diaphragm performance values

Diaphragm	F_y (kN)	Δ_y (mm)	F_{ult} (kN)	Δ_{ult} (mm)	K_1 (kN/m)	K_2 (kN/m)	R_d (kN/m)	G_d (kN/m)	μ (ratio)
1a-PARA	17.2	26.8	36.8	193.0	644	159	1.6	198	7.2
1b-PARA	175.8	12.1	175.8	149.9	14,518	0	15.9	4459	12.4
2a-PARA	17.7	29.4	35.9	197.0	601	151	1.6	185	6.7
2b-PARA	171.9	12.5	171.9	127.9	13,768	0	15.5	4229	10.2
1a-PERP	27.0	16.9	102.9	148.7	1605	569	1.3	134	8.8
1b-PERP	204.7	9.1	204.7	132.6	22,409	0	9.8	1864	14.6
2a-PERP	30.2	16.7	99.1	148.6	1743	517	1.5	145	8.9
2b-PERP	192.6	6.4	192.6	132.7	29,960	0	9.3	2493	20.6

TABLE 3: Retrofit serviceability performance

Diaphragm						Serviceability limits	
	F_e (kN)	F_y (kN)	μ_{demand} (ratio)	Δ_y (mm)	Δ_{demand} (mm)	Δ_{L1} (mm)	Δ_{L2} (mm)
1b-PARA	524	175.8	2.98	12.1	36.1	25	100
2b-PARA	524	171.9	3.04	12.5	38.0	25	75
1b-PERP	289	204.7	1.41	9.1	12.8	15	75
2b-PERP	289	192.6	1.50	6.4	9.6	15	75

TABLE 4: Comparison with predicted performance using current assessment documents

	Strength, F_y (kN)			Yield displacement, Δ_y (mm)			Stiffness, K_d (kN/m)		
	NZSEE	ASCE	Exp	NZSEE	ASCE	Exp	NZSEE	ASCE	Exp
1a-PARA	15.5	19.4	17.2	74.9	13.8	26.8	207	745	644
2a-PARA	15.5	19.4	17.7	74.9	13.8	29.4	207	745	601
1a-PERP	29.1	36.4	27.0	39.8	26.0	16.9	730	2630	1605
2a-PERP	29.1	36.4	30.2	39.8	26.0	16.7	730	2630	1743

LIST OF FIGURES

FIGURES

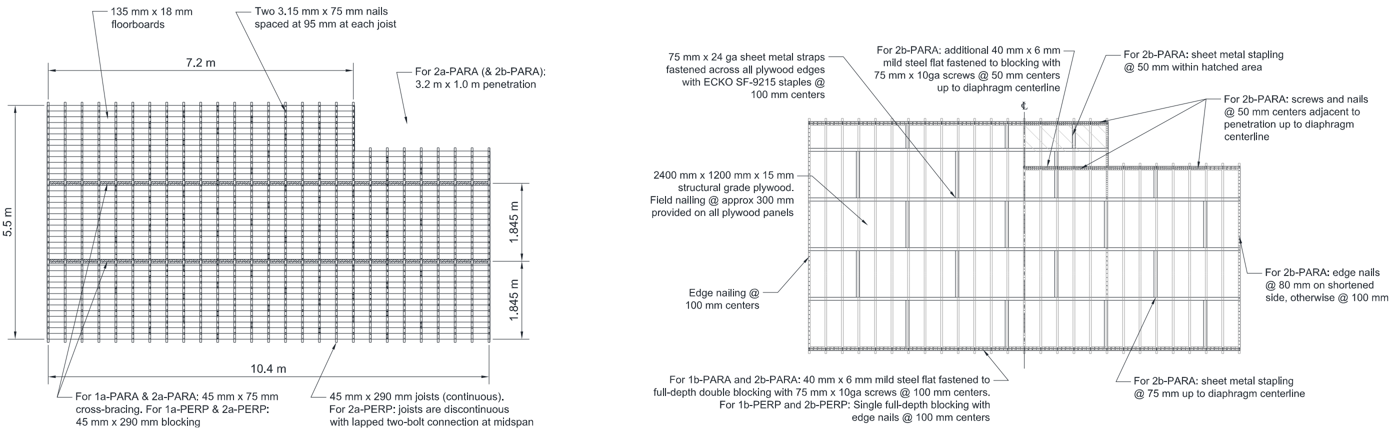

(a) As-built configurations

(b) Retrofitted configurations

FIG. 1: As-built and retrofitted diaphragm configuration examples

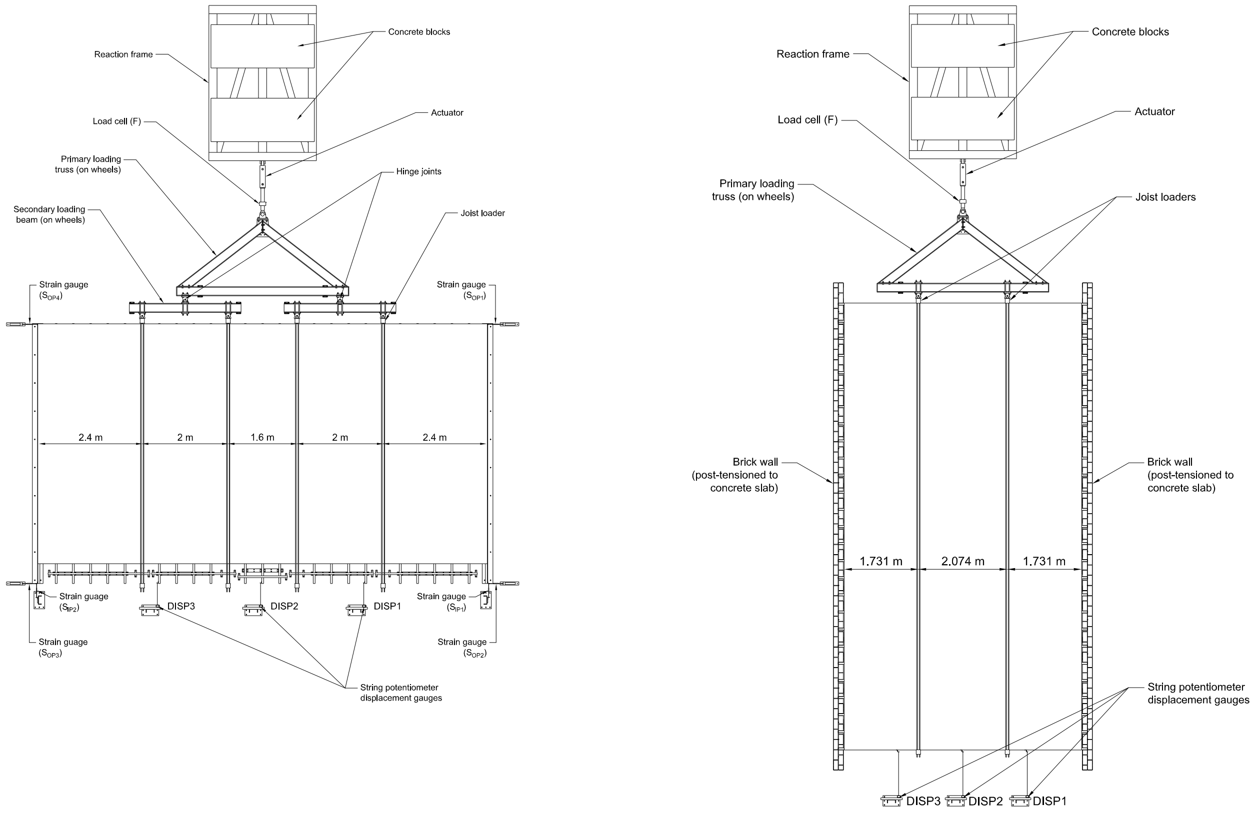

(a) Parallel-to-joist loading

(b) Perpendicular-to-joist loading

FIG. 2: Test set-up

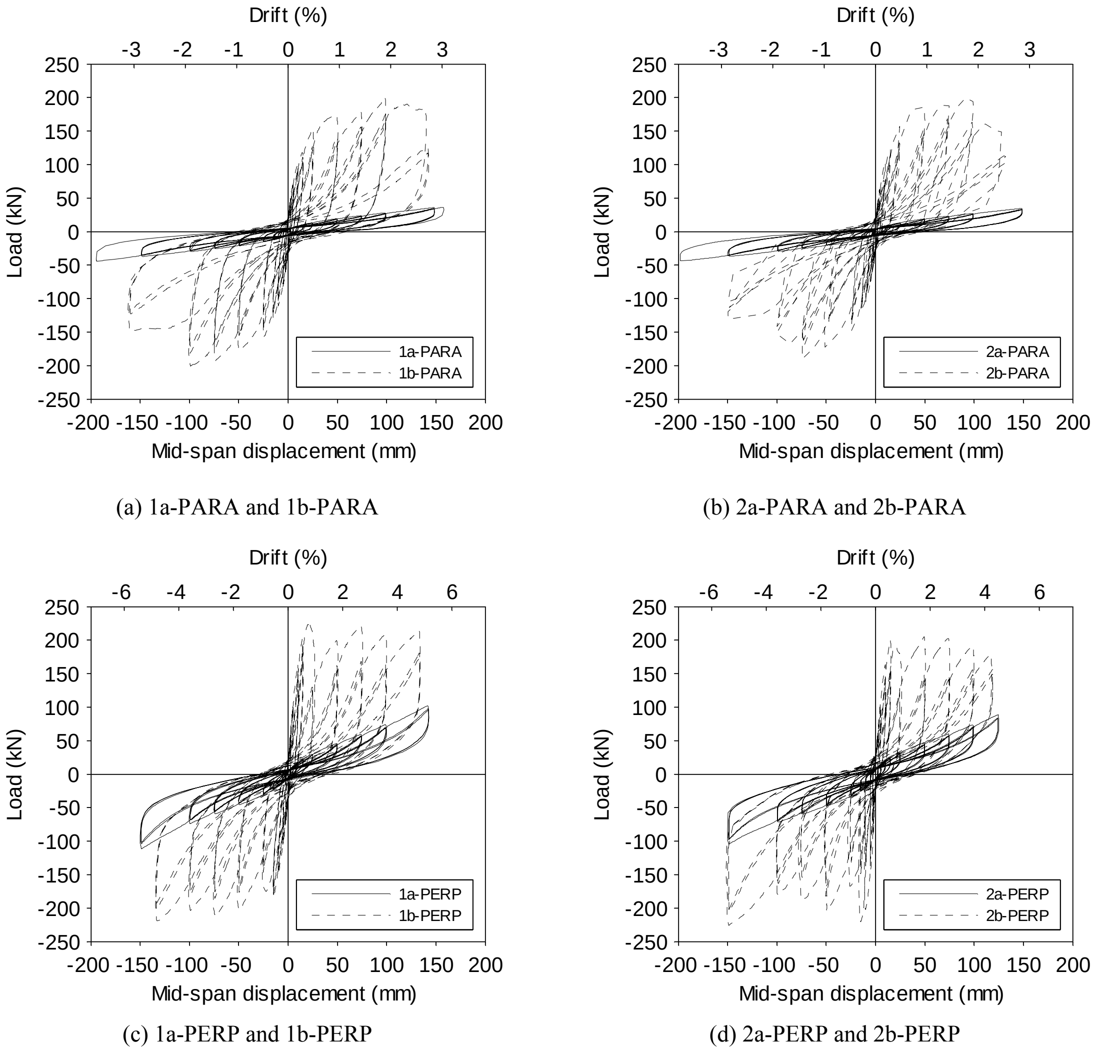

(a) 1a-PARA and 1b-PARA

(b) 2a-PARA and 2b-PARA

(c) 1a-PERP and 1b-PERP

(d) 2a-PERP and 2b-PERP

FIG. 3: Force-displacement responses of diaphragms

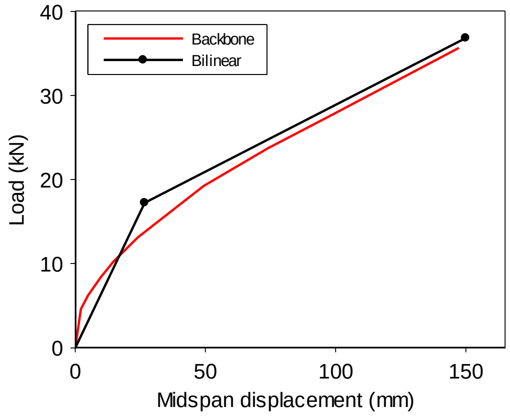

FIG. 4: Backbone of 1a-PARA for positive displacements only

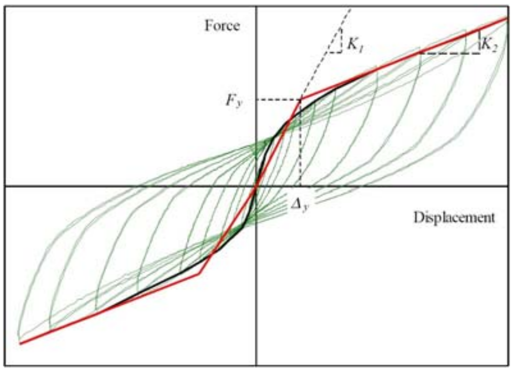

(a) As-built diaphragms [modified from Peralta et al. (2004)]

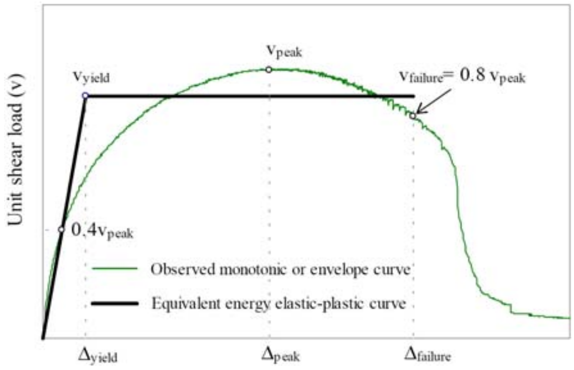

(b) Retrofitted diaphragms [reproduced from Salenikovich (2000)]

FIG. 5: Bilinear representations of diaphragm backbone response curves

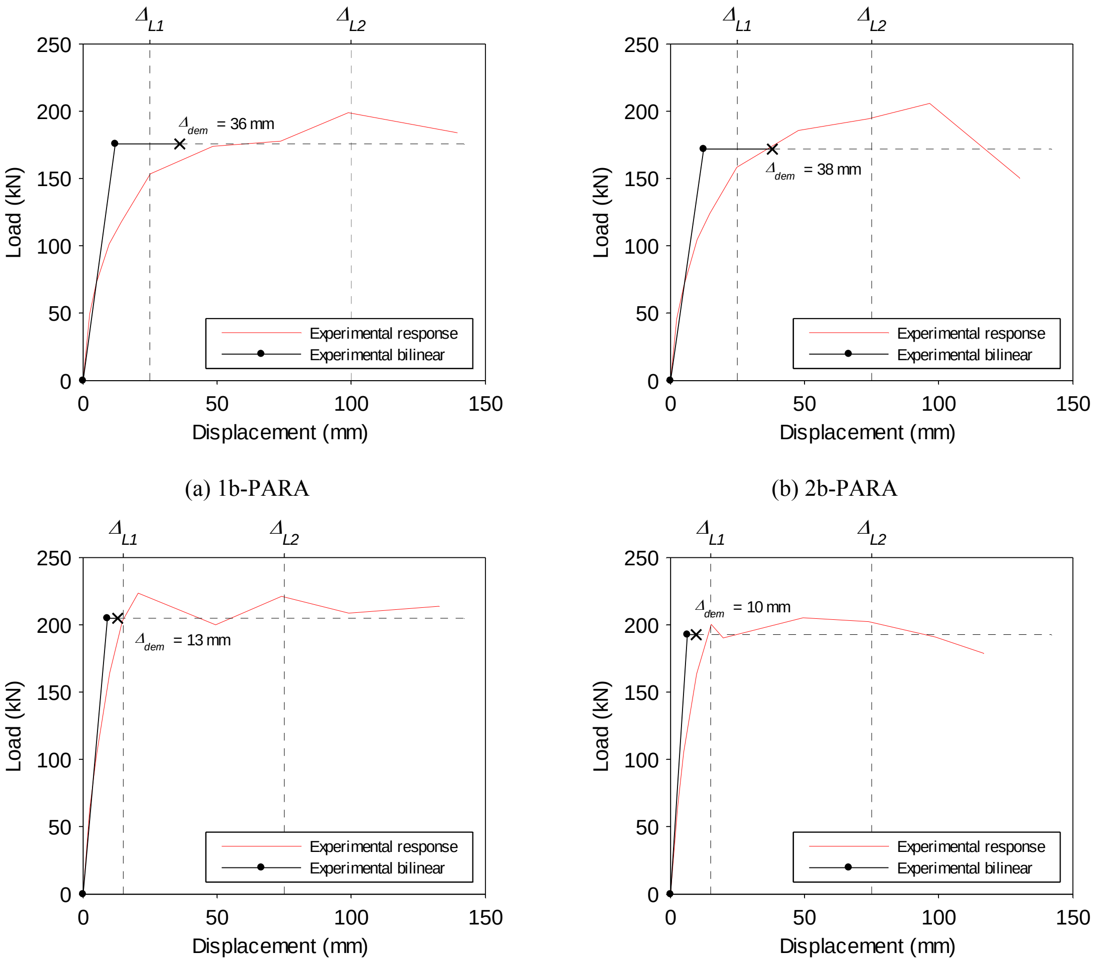

(a) 1b-PARA

(b) 2b-PARA

(c) 1b-PERP

(d) 2b-PERP

FIG. 6: Retrofit serviceability performance